

Stable two-channel Kondo fixed point of an SU(3) quantum defect in a metal: renormalization group analysis and conductance spikes

Michael Arnold, Tobias Langenbruch and Johann Kroha
Physikalisches Institut, Universität Bonn, Nussallee 12, 53115 Bonn, Germany
 (Dated: February 1, 2008)

We propose a physical realization of the two-channel Kondo (2CK) effect, where a dynamical defect in a metal has a unique ground state and twofold degenerate excited states. In a wide range of parameters the interactions with the electrons renormalize the excited doublet downward below the bare defect ground state, thus stabilizing the 2CK fixed point. In addition to the Kondo temperature T_K this system exhibits another low-energy scale, associated with ground-to-excited-state transitions, which can be exponentially smaller than T_K . Using the perturbative nonequilibrium renormalization group we demonstrate that this can provide the long-sought explanation of the sharp conductance spikes observed by Ralph and Buhrman in ultrasmall metallic point contacts.

PACS numbers: 72.10.Fk, 72.15.Qm 73.63.Rt

The two-channel Kondo (2CK) effect has been intriguing physicists ever since it was proposed by Nozières and Blandin in 1980 [1] because of its exotic non-Fermi liquid ground state with a nonvanishing zero-point entropy $S(0) = k_B \ln \sqrt{2}$ [2]. It arises when a discrete, degenerate quantum degree of freedom is exchange-coupled to two conserved conduction electron continua or channels in a symmetrical way [3]. Early on, Vlášar and Zawadowski [4] put forward two-level systems (TLS), e.g. an atom in a double well potential embedded in a metal, as a physical realization of a 2CK system. However, this model encountered difficulties because for small exchange coupling, $J \ll 1/N(0)$, with $N(0)$ the conduction density of states at the Fermi energy, the renormalized level splitting of the TLS cannot become less than the exponentially small Kondo temperature, $T_K \sim \exp[-1/(4N(0)J)]$, and a large effective coupling, $N(0)J \approx 1$, cannot be realized even by invoking enhanced electron assisted tunneling via virtually excited states of the TLS [5] because of cancellation [6] and screening [7] effects. It remains difficult to reach by a resonance enhancement of $N(0)$ proposed in Ref. [8].

Signatures of the 2CK effect have been observed experimentally in heavy fermion compounds [9] and most recently in especially designed quantum dot systems [10]. However, perhaps the most intense interest has been provoked by the conductance anomalies observed by Ralph and Buhrman [11] in ultrasmall metallic point contacts. This is because, on the one hand, these measurements showed most clear-cut 2CK signatures near zero bias, including the theoretically expected [12, 13] scaling behavior [14], and, on the other hand, these zero-bias anomalies (ZBA) occurred in seemingly simple Cu point contacts. In addition, sharp spikes were observed in the conductance at elevated bias [11], such that contacts with conductance spikes always exhibited also the ZBA. These results have remained essentially not understood to the

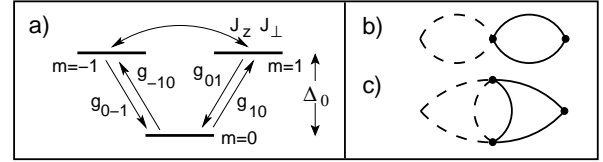


FIG. 1: a) Level scheme of the three-state defect, defining the coupling constants in Eq. (1); b) 2nd and c) 3rd order contributions to the current through a point contact with Kondo impurities. — : conduction electron, - - - : defect state propagators. A • indicates a sum over all 4-point vertices of Eq. (1).

present day mainly due to the lack of a microscopic model with a stable 2CK fixed point, although some of the features could alternatively be accounted for by a distribution of TLS without invoking the 2CK effect [15]. However, a reliable understanding requires an explanation of all the experimental features. The difficulty resides in the fact that in the usual 2CK models the Kondo SU(2) symmetry is easily destroyed by relevant perturbations.

In this Letter we present a realistic, microscopic model for the 2CK effect, where the Kondo degree of freedom are the parity-degenerate rotational states ($m = \pm 1$) of an atomic three-level system (3LS) and the channel degree of freedom is the magnetic conduction electron spin. Such a level scheme (see Fig. 1) is generically realized by an atom (hydrogen ion) moving in a modulated Mexican hat potential which, e.g., is formed in the interstitial space of the (111) plane of a Cu lattice. Although similar models have been considered before [16, 17], they have not been analyzed in detail, especially not in a current-carrying, finite bias situation [18, 19, 20]. We show that for a wide range of parameters the 2CK fixed point is stabilized by a correlation-induced level crossing, forcing the degenerate defect levels to be the interacting ground states of the defect. In addition to the 2CK Kondo temperature T_K , the 3LS has another correlation-induced

low-energy scale T_K^* , associated with ground-to-excited-state transitions. T_K^* can be exponentially smaller than T_K . We show by explicit renormalization group (RG) calculations of the non-equilibrium differential conductance [18, 19] that this can account for conductance spikes at elevated bias, much narrower than the ZBA.

The model. — For the defect levels we employ the Abrikosov pseudospin representation, where f_m^\dagger is the creation operator for the defect in state $m = 0, \pm 1$, $m = 0$ labeling the (non-interacting) ground state and $m = \pm 1$ the excited doublet [cf. Fig. 1a)]. The defect dynamics are subject to the constraint $\hat{Q} = \sum_{m=0,\pm 1} f_m^\dagger f_m = 1$. The defect coupled to the conduction electron continuum is then described by the Hamiltonian,

$$H = \sum_{\mathbf{k}\sigma m\alpha} \varepsilon_{\mathbf{k}} c_{\mathbf{k}\sigma m}^\alpha \dagger c_{\mathbf{k}\sigma m}^\alpha + \Delta_0 \sum_{m=\pm 1} f_m^\dagger f_m + \sum_{\sigma\alpha\beta} \left[\frac{J_z}{2} S_z s_z^{\sigma\alpha\beta} + J_\perp \left(S_{1,-1} s_{-1,1}^{\sigma\alpha\beta} + S_{-1,1} s_{1,-1}^{\sigma\alpha\beta} \right) \right] + \sum_{\mathbf{k}\mathbf{k}'} \sum_{\sigma\alpha\beta} \sum_{\substack{m,n \\ -1 \leq n-m \leq 1}} \left[g_{m0}^{(n)} S_{m,0} s_{n-m,n}^{\sigma\alpha\beta} + H.c. \right], \quad (1)$$

where the first term represents the conduction electron kinetic energy, the second one the degenerate local doublet with level splitting Δ_0 above the defect ground state, and the third and fourth terms transitions between the local levels induced by conduction electron scattering, see Fig. 1a). The conduction electron operators, $c_{\mathbf{k}\sigma m}^\alpha$, carry the conserved magnetic spin $\sigma = \pm 1/2$ as well as an SU(3) index $m = 0, \pm 1$ which is altered by the defect scattering, and which is thought to be associated with an electronic orbital degree of freedom centered around the defect. The prime in the kinetic energy indicates a restricted momentum sum such that $\sum_{\mathbf{k}m} \equiv \sum_{\mathbf{k}}$ covers the complete momentum space. Note that in the rotational defect model the effective band cut-off reduction of Ref. [7] due to screening by high-energy electrons does not occur, because the transitions $m = 1 \leftrightarrow m = -1$ are not associated with a charge redistribution. For later use we assume that the defect is located in a nanoscopic point contact between two metallic leads held at chemical potentials $\mu_\pm = \mu \pm V/2$ [11]. The electron distribution function at the location of the defect is then $f(\omega) = [f_0(\omega + V/2) + f_0(\omega - V/2)]/2$, with $f_0(\omega)$ the Fermi distribution function. Throughout, Greek superscripts $\alpha, \beta = \pm$ indicate whether an electron is from the high (μ_+) or the low (μ_-) potential reservoir. The defect SU(3) operators are defined as $S_z = f_1^\dagger f_1 - f_{-1}^\dagger f_{-1}$, and

$S_{mn} = f_m^\dagger f_n$, and the SU(3) operators acting on the electronic Fock space, s_z, s_{mn} , are obtained by substituting $f_m \rightarrow \sum_{\mathbf{k}} c_{\mathbf{k}\sigma m}^\alpha$ in the above expressions. In Eq. (1) we have chosen a representation of SU(3) which explicitly exhibits the unbroken symmetry of the SU(2) subgroup in the states $m = \pm 1$. In the following we use dimensionless couplings denoted by the identification $N(0)g_{mn}^{(j)} \rightarrow g_{mn}^{(j)}$.

Nonequilibrium RG. — The defect is described by the (retarded) impurity propagator $G_m(\nu) = [\nu - |m|\Delta + i\Gamma_m]^{-1}$, which, by symmetry, remains diagonal in m , even when coupled to the electron system. Here Δ is the renormalized level-spacing (see below), and Γ_m is the interaction-induced decay rate of level m . When a bias voltage V is applied, all electrons within at least the voltage window contribute to the scattering. The corrections to the electron-defect vertex depend on the energy of the incoming electron, ω , and of the in- and out-going defect states n, m . To a very good approximation [18], the defect dynamics can be taken on-shell ($\nu = |m|\Delta$), so that the electron-defect vertex depends on n, m , and on ω as the only continuous variable. This has led in Ref. [18] to the concept of a perturbative RG for coupling functions, parameterized by the energy of the incoming electron, i.e. the Hamiltonian, considered at each electron energy ω , has its own RG flow. The one-loop RG equations for our SU(3) model can be derived as [18],

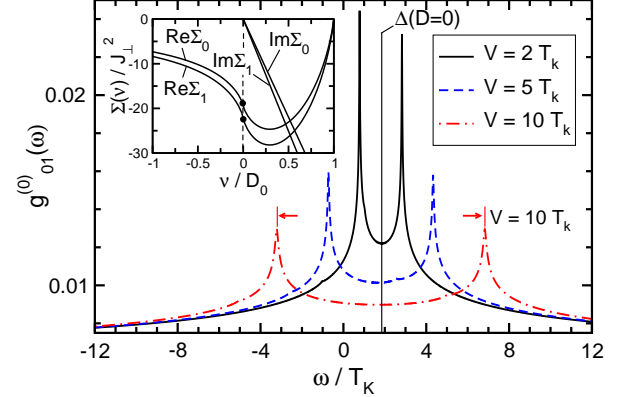


FIG. 2: (Color online) Coupling function $g_{01}^{(0)}(\omega)$ for different bias voltages V (parameter values as in Fig. 3). The peak structure of $g_{01}^{(0)}(\omega)$ is centered around the renormalized level spacing $\Delta(D=0)$ and is split by the respective bias V . The inset shows the defect selfenergy $\Sigma_m(\omega)$, $m = 0, 1$, calculated in bare 2nd order PT. The level spacing renormalization is the difference between the two solid dots, $\delta\Delta = \text{Re}(\Sigma_1(\Delta) - \Sigma_0(\Delta))$.

$$\frac{dg_{mn}^{(j)\alpha\beta}(\omega)}{d\ln D} = 2 \sum_{\substack{j\ell\gamma \\ -1 \leq j+n-\ell \leq 1}} g_{m\ell}^{(j+n-\ell)\alpha\gamma}(\Omega_{n\ell}) g_{\ell n}^{(j)\gamma\beta}(\omega) \Theta\left(D - \sqrt{\left(\Omega_{n\ell} - \frac{\gamma V}{2}\right)^2 + \Gamma_\ell^2}\right) (1 - \delta_{m\ell}\delta_{n\ell}) - \text{exch.} \quad (2)$$

with $g_{1,-1}^{(1)} = g_{-1,1}^{(-1)} = J_\perp$ and $g_{mm}^{(j)} = jmJ_z/2$, for $j = \pm 1, m = \pm 1$. The Θ step function in Eq. (2) controls that the RG flow of a particular term is cut off when the band cutoff D , symmetrical about the Fermi edge $\gamma V/2$ in lead $\gamma = \pm$, is reduced below the energy of the intermediate scattering electron in that lead. This energy is $\Omega_{n\ell} = \omega + (|n| - |\ell|)\Delta(D)$. The Kronecker- δ factor excludes non-logarithmic terms which do not alter the impurity state. The energy arguments of the g 's on the right-hand-side (RHS) arise from energy conservation at each vertex. The exchange terms, exch. , on the RHS of Eq. (2) are obtained from the direct ones by interchanging in the g 's in- and out-going pseudofermion indices and by interchanging $m \leftrightarrow n$ everywhere. The RHS also contains the decay rates Γ_m [18] and the renormalized level spacing Δ . Although Γ_m and Δ contain no leading logarithmic terms, they acquire an RG flow, since they are calculated in 2nd order Keldysh perturbation theory (PT) using the running couplings $g_{mn}^{(j)}(\omega)$ [18, 19]. Specifically, Δ is obtained during the RG flow as,

$$\Delta = \Delta_0 + \text{Re}\Sigma_1(\nu = \Delta) - \text{Re}\Sigma_0(\nu = 0), \quad (3)$$

We find no significant V -dependence of Δ for $\ln(V/D_0) \ll 1$. Note that the renormalized g 's have, in general, different ω dependence, even if their bare values are chosen equal. The typical behavior of the coupling functions as solutions of Eq. (2) for $D \rightarrow 0$ is shown in Fig. 2 for $g_{01}^{(0)}(\omega)$ as an example. As expected for resonant transitions from the excited to the impurity ground state, $g_{01}^{(0)}(\omega)$ has a peak structure centered around the renormalized transition energy Δ . The peak is cut off by Γ_m and split by the applied bias, reflecting the difference between the Fermi levels in the two leads. The Kondo temperature T_K has been determined here and throughout as the cutoff value D for which the coupling reaches $J_\perp(\omega = \pm V/2) = 1$.

Equilibrium: 2CK fixed point. — To investigate the fixed point structure of the model (1), we first analyze the RG flow in equilibrium at temperature $T = 0$. The Greek superscripts have then no relevance. Note that even for $V = 0$ the renormalized couplings have an ω -dependence. However, in this case it is sufficient to consider electrons at the Fermi level only, $\omega = 0$ and $\Gamma_m = 0$. Due to time reversal symmetry we have in equilibrium, $g_{mn}(\omega) = g_{nm}(\omega + (|n| - |m|)\Delta)$. We have checked that for $V = 0$ the results of the RG equations (2) coincide with those of the familiar equilibrium perturbative RG. As the most important point of this paper we find that the level spacing Δ is always renormalized downward by the RG flow and, for a wide range of bare parameters J_z , J_\perp , Δ_0 , and g , crosses the impurity ground level. Such a crossing is not forbidden by symmetry, since even for completely symmetric initial couplings they have already been renormalized to different values when the level crossing occurs. Typical RG flow curves $\Delta(\ln D)$

are shown in the inset of Fig. 3. It is seen that the level crossing occurs generically in the regime $\ln(D/T_K) \gg 1$, where the perturbative RG treatment is still controlled. Hence, this behavior can qualitatively be understood by 2nd order PT as follows (cf. Fig. 2, inset). The imaginary part of the defect selfenergy $\Sigma_m(\nu)$ is well known to have threshold behavior with $\text{Im}\Sigma_m(\nu < 0) = 0$ [21]. Because of resonant transitions between the degenerate states $m = \pm 1$ one has always $|\text{Im}\Sigma_1(\nu)| > |\text{Im}\Sigma_0(\nu)|$, so that via Kramers-Kronig the level spacing renormalization in Eq. (3), $\text{Re}[\Sigma_1(\Delta) - \Sigma_0(0)]$ is necessarily negative (the difference between the black dots in Fig. 2, inset). We find that even in bare 2nd order PT for $\Sigma_m(\nu)$ the renormalization may be stronger than the bare spacing Δ_0 , thus inducing a level crossing. Once the level crossing has occurred, the system is bound to flow to a stable 2CK fixed point, since the renormalized ground state of the local defect is now doubly degenerate (Kondo degree of freedom), stabilized by spatial parity of the underlying crystal lattice, and the channel symmetry of the magnetic electron spin is preserved by Kramers degeneracy. Our results are summarized in the equilibrium phase diagram shown in Fig. 3. The 2CK phase is realized for a sizable range of parameters.

Nonequilibrium differential conductance. — Finally we compute the current through an ultrasmall metallic point contact in the presence of 2CK defects. We assume that a conductance channel is blocked when a 2CK scattering from that channel occurs. The current correction due to a single 2CK defect is then $\delta I(V) = -\frac{e}{h} \langle [(\rho_+ - \rho_-), H] \rangle$, with $\rho_\alpha = \sum_{\mathbf{k}\sigma m} c_{\mathbf{k}\sigma m}^\dagger c_{\mathbf{k}\sigma m}$. We computed this expres-

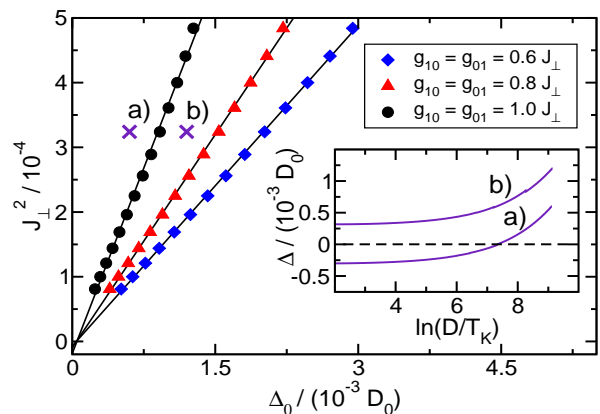


FIG. 3: (Color online) Phase diagram in the $J_\perp^2 - \Delta_0$ plane for $J_z/2 = J_\perp = 0.018$, bias $V = 0$, and various values of $g_{0m}^{(n)} = g_{m0}^{(n)}$, $n, m = 0, \pm 1$. The symbols mark the line of instable fixed points separating the 2CK (left of the line) from the potential scattering (right of the line) low-temperature phase. The solid lines are straight line fits to the J_\perp^2 vs. Δ_0 plots and show that the level crossing is essentially an $O(J_\perp^2)$ PT effect. The inset shows typical RG flow diagrams of the level spacing $\Delta(D)$ in a) the 2CK phase (level crossing) and b) the potential scattering phase (no level crossing).

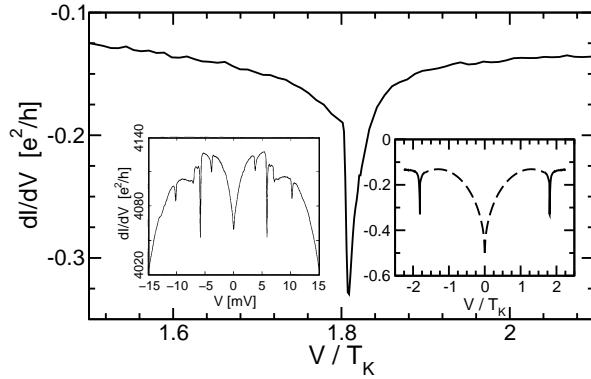


FIG. 4: Differential conductance correction dI/dV per defect for bias V near the renormalized level spacing $\Delta(D = 0)$, $V > T_K \approx 10^{-4} D_0$. $J_z/2 = J_\perp = 0.016$, $g_{01}^{(j)} = g_{10}^{(j)} = 0.6J_\perp$, $\Delta_0 = 3T_K$, $\Delta(D = 0) = -1.82T_K$. Right inset: dI/dV for a larger bias range. The dashed line is a sketch of the 2CK-induced $\sqrt{|V|}$ -ZBA of width T_K , with the numerically determined T_K , as indicated. Left inset: Experimental dI/dV curve taken from Ref. [11] for comparison.

sion for $T = 0$, as outlined in Ref. [18], by evaluating the 2nd order Keldysh diagram shown in Fig. 1b) [19], using the renormalized coupling functions obtained from Eq. (2), and obtained the voltage dependent nonequilibrium conductance dI/dV . Details of the lengthy calculation will be presented elsewhere. The results are displayed in Fig. 4, showing conductance spikes much narrower than T_K at a bias V corresponding to the renormalized level spacing for that bias, $V = \pm|\Delta|$. These spikes, with a steep step on the low- V side and a wider (logarithmic) decay on the high- V side, are analogous to the conductance peaks of a Kondo quantum dot in a magnetic field [18]. They are due to transitions between the (renormalized) ground- and excited-state defect levels, enhanced by Kondo scattering. Despite their complicated shape arising from a combination of many terms, their overall narrow width can be understood from the fact that the model (1) contains at least one more low-energy scale in addition to T_K : While T_K is to leading log order determined by fluctuations between the *degenerate* defect levels ($m = \pm 1$), i.e. by J_\perp , $T_K \simeq D_0 \exp[-1/4J_\perp]$, the conductance has in 3rd order [cf. Fig. 1c)] a logarithmic divergence at $V = \pm|\Delta|$, which is governed by the couplings $g_{10}^{(1)} = g_{-10}^{(-1)}$, $dI/dV \simeq 4g_{10}^{(1)} \ln[\Theta(|V| - |\Delta|)(|V| - |\Delta|)/D_0]$. The width of this peak, although additionally cut off by the nonequilibrium rates Γ_m , may thus be estimated as $T_K^* \simeq D_0 \exp[-1/4g_{10}^{(1)}]$, i.e. for $g_{10}^{(1)} < J_\perp$ it is exponentially smaller than T_K [23].

In conclusion, we have shown that a three level defect with partially broken $SU(3)$ symmetry and degenerate excited states in a metal has a sizable, stable 2CK fixed point phase and that this model can describe conductance spikes exponentially more narrow than T_K . Hence,

the model suggests a unified microscopic explanation for the essential features of the conductance anomalies observed by Ralph and Buhrman [11]. The reduction of the ZBA and the splitting of the spikes in a magnetic field B [11] can be explained by a coupling of B to the defect angular momentum and the resulting Zeeman splitting of the levels $m = \pm 1$. This will be discussed elsewhere. The size of the anomalies $\sim 100 e^2/h$ might be due to a corresponding number of 2CK defects in the contact. The very sharp experimental distribution of T_K [11] may occur, because the rotational defects form at equivalent interstitial sites in a (nearly perfect) Cu lattice or because only those defects with sufficiently high T_K are observable [22]. — We wish to thank J. von Delft, A. Rosch, and especially A. Zawadowski for numerous useful discussions. This work was supported by DFG through SFB 608 and grant No. KR1726/1.

-
- [1] P. Nozières and A. Blandin, *Journal de Physique (Paris)*, **41**, 193 (1980).
 - [2] N. Andrei and C. Destri, *Phys. Rev. Lett.* **52**, 364 (1984); A. M. Tsvelik and P. B. Wiegmann, *Z. Phys. B* **54**, 201 (1994).
 - [3] D. L. Cox and A. Zawadowski, *Adv. Phys.* **47**, 599 (1998).
 - [4] K. Vladár and A. Zawadowski, *Phys. Rev. B* **28**, 1564 (1983); **28**, 1582 (1983); *Phys. Rev. B* **28**, 1596 (1983).
 - [5] G. Zaránd and A. Zawadowski, *Phys. Rev. Lett.* **72**, 542 (1994); *Phys. Rev. B* **50**, 932 (1994).
 - [6] I. L. Aleiner *et al.*, *Phys. Rev. Lett.* **86**, 2629 (2001).
 - [7] I. L. Aleiner and D. Controzzi, *Phys. Rev. B* **66**, 045107 (2002).
 - [8] G. Zaránd, *Phys. Rev. B* **72**, 245103 (2005).
 - [9] C. L. Seaman *et al.*, *Phys. Rev. Lett.* **67**, 2882 (1991); T. Cichorek *et al.*, *Phys. Rev. Lett.* **94**, 236603 (2005).
 - [10] R. M. Potok *et al.*, *Nature* **446**, 167 (2007).
 - [11] D. C. Ralph and R. A. Buhrman, *Phys. Rev. Lett.* **69**, 2118 (1992); *Phys. Rev. B* **51**, 3554 (1995).
 - [12] I. Affleck and A. W. W. Ludwig, *Nucl. Phys. B*, **352**, 849 (1991); *Phys. Rev. B* **48**, 7297 (1993).
 - [13] M. H. Hettler, J. Kroha, and S. Hershfield, *Phys. Rev. Lett.* **73**, 1967 (1994).
 - [14] D. C. Ralph, A. W. W. Ludwig, J. von Delft, and R. A. Buhrman, *Phys. Rev. Lett.* **75**, 770 (1995).
 - [15] V.I. Kozub and A.M. Rudin, *Phys. Rev. B* **55**, 259 (1997).
 - [16] A. L. Moustakas and D. S. Fisher, *Phys. Rev. B* **55**, 6832 (1997).
 - [17] G. Zaránd, *Phys. Rev. Lett.* **77**, 3609 (1996); A. Jerez, N. Andrei, and G. Zaránd, *Phys. Rev. B* **58**, 3814 (1998).
 - [18] A. Rosch, J. Paaske, J. Kroha, and P. Wölfe, *Phys. Rev. Lett.* **90**, 076804 (2003).
 - [19] J. Paaske, A. Rosch, and P. Wölfe, *Phys. Rev. B* **69**, 155330 (2004).
 - [20] J. Paaske, A. Rosch, J. Kroha, and P. Wölfe, *Phys. Rev. B* **70**, 155301 (2004).
 - [21] See, e.g., T. A. Costi, J. Kroha, and P. Wölfe *Phys. Rev. B* **53**, 1850 (1996).
 - [22] Ch. Kolf and J. Kroha, *Phys. Rev. B* **75**, 045129 (2007).
 - [23] In case $\Gamma_m(V) > T_K^*$, the peak width is controlled by $\Gamma_m(V)$ and may be significantly larger than T_K .